

UCLA

UCLA Previously Published Works

Title

Macular Ganglion Cell/Inner Plexiform Layer Measurements by Spectral Domain Optical Coherence Tomography for Detection of Early Glaucoma and Comparison to Retinal Nerve Fiber Layer Measurements

Permalink

<https://escholarship.org/uc/item/3qk3806b>

Journal

American Journal of Ophthalmology, 156(6)

ISSN

0002-9394

Authors

Nouri-Mahdavi, Kouros
Nowroozizadeh, Sara
Nassiri, Nariman
et al.

Publication Date

2013-12-01

DOI

10.1016/j.ajo.2013.08.001

Peer reviewed

Published in final edited form as:

Am J Ophthalmol. 2013 December ; 156(6): . doi:10.1016/j.ajo.2013.08.001.

Macular Ganglion Cell/Inner Plexiform Layer Measurements with Spectral Domain Optical Coherence Tomography for Detection of Early Glaucoma and Comparison to Retinal Nerve Fiber Layer Measurements

Kouros Nouri-Mahdavi, MD MSc, Sara Nowroozizadeh, MD, Nariman Nassiri, MD MPH, Nila Cirineo, MD, Shane Knipping, BS, JoAnn Giaconi, MD, and Joseph Caprioli, MD
Glaucoma Division, Jules Stein Eye Institute, David Geffen School of Medicine, University of California Los Angeles

Abstract

Purpose—To evaluate the performance of ganglion cell/inner plexiform layer (GC/IPL) measurements with spectral-domain optical coherence tomography (Cirrus HD-OCT) for detection of early glaucoma and to compare results to retinal nerve fiber layer (RNFL) measurements.

Design—Cross-sectional prospective diagnostic study.

Methods—Fifty-nine glaucoma eyes (47 subjects) (mean deviation >-6.0 dB) and 91 normal eyes (52 subjects) were enrolled. Patients underwent biometry and peripapillary and macular OCT imaging. Performance of the GC/IPL and RNFL algorithms was evaluated with area under receiver operating characteristic curves (AUC), likelihood ratios, and sensitivities/specificities adjusting for covariates. Combination of best parameters was explored.

Results—Average (SD) mean deviation in the glaucoma group was -2.5 (1.9) dB. On multivariate analyses, age ($p<0.001$) and axial length ($p=0.03$) predicted GC/IPL measurements in normal subjects. No significant correlation was found between average or regional GC/IPL thickness and respective outer retina (OR) thickness measurements ($p>0.05$). Average RNFL thickness performed better than average GC/IPL measurements for detection of glaucoma (AUC=0.964 vs. 0.937; $p=0.04$). The best regional measures from each algorithm (inferior quadrant RNFL vs. minimum GC/IPL) had comparable performances ($p=0.78$). Entering GCIPL/OR ratio into prediction models did not enhance performance of the GC/IPL measures. Combining the best parameters from each algorithm improved detection of glaucoma ($p=0.04$).

Conclusions—Regional GC/IPL measures derived from Cirrus HD-OCT performed as well as regional RNFL outcomes for detection of early glaucoma. Using GCIPL/OR ratio did not enhance

© 2013 Elsevier Inc. All rights reserved.

Corresponding author: Kouros Nouri-Mahdavi, MD MSc, 100 Stein Plaza, Los Angeles CA 90095 Phone: 310-794-1487 Fax: 310-794-6616 nouri-mahdavi@jsei.ucla.edu.

Publisher's Disclaimer: This is a PDF file of an unedited manuscript that has been accepted for publication. As a service to our customers we are providing this early version of the manuscript. The manuscript will undergo copyediting, typesetting, and review of the resulting proof before it is published in its final citable form. Please note that during the production process errors may be discovered which could affect the content, and all legal disclaimers that apply to the journal pertain.

Contributions to Authors: Involved in conception and design of study (K.N.); Analysis and interpretation (K.N., S.N.); Writing the article (K.N., S.N.); Critical revision of the article (J.G., J.C.); Final approval of the article (K.N., S.N., N.N., N.C., S.K., J.G., J.C.); Data collection (K.N., S.N., N.N., N.C., S.K.); Provision of materials, patients, or resources (K.N., J.G., J.C.); Statistical expertise (K.N.); Obtaining funding (K.N.); Literature search (K.N.); Administrative, technical, or logistic support (S.K.).

the performance of GC/IPL parameters. Combining the best measures from the two algorithms improved detection of glaucoma.

Introduction

The hallmark of glaucoma is loss of the retinal ganglion cell axons that leads to a typical optic neuropathy. Qualitative and quantitative evaluation of the optic nerve head (ONH) and/or retinal nerve fiber layer (RNFL) has been used to detect evidence of glaucomatous damage. There is evidence that macular ganglion cell loss can be demonstrated in early experimental glaucoma.¹ In addition, recent publications suggest that evidence of glaucomatous damage can be observed in the inner retina or ganglion cell complex (GCC), i.e. the combined thickness of the RNFL, ganglion cell layer (GCL), and inner plexiform layer (IPL), early during the disease process with spectral domain optical coherence tomography (SD-OCT).^{2,3} A recent study showed that GCC loss could be detected in eyes with preperimetric glaucoma.⁴ It has been suggested that the macular GC layer thickness may be the most relevant parameter to measure in glaucoma.⁵ However, given the resolution of the current generation of SD-OCTs, accurate measurement of the GCL alone is not practical. Hence, some SD-OCT manufacturers have developed segmentation algorithms for calculating the GCC thickness or the combined thickness of the GCL and IPL. The software versions 6.0 or higher of Cirrus High-Definition OCT (Cirrus HD-OCT, Carl Zeiss Meditec, Dublin CA) now provide a Ganglion Cell Analysis where GC/IPL thickness measurements and various graphical and statistical analyses are provided. There is preliminary evidence that such GC/IPL measurements may perform as well as RNFL measures for detection of early glaucoma.^{6,7} Prior studies have reported age and axial length as the main factors affecting variability of the GC/IPL or GCC measurements.^{8,9} A recent study found that the GCC/total retinal thickness ratio performed better than all other RNFL or macular parameters for detection of glaucoma.¹⁰ This finding, if confirmed, suggests that the thickness of the inner retinal tissues is related to the density and thickness of the outer retinal cells and therefore, the ratio of the inner to outer retinal layers may be a useful parameter to include in algorithms used for detection of glaucoma. The goal of the current study is to explore factors affecting the GC/IPL thickness in a group of normal eyes from the UCLA OCT Imaging Study, to evaluate the performance of the newly defined GC/IPL measurements for detection of early glaucoma, and to compare the findings to RNFL thickness measurements. We also hypothesized that the outer retina thickness may predict the GC/IPL thickness and hence including the OR thickness or the GCIPL/OR ratio in the prediction models using macular measurements may improve their performance.

Methods

This study was approved by the Institutional Review Board at the University of California Los Angeles (UCLA) and was carried out in accordance with the Declaration of Helsinki. Fifty-nine eyes of 47 glaucoma subjects and 91 eyes of 52 normal subjects were prospectively recruited between December 2010 and October 2012. Patients with a clinical diagnosis of open-angle glaucoma made by an attending ophthalmologist were prospectively identified and invited to be enrolled in the study if they met the following criteria: age ≥ 30 years, open angles, visual acuity $\geq 20/80$, visual field mean deviation ≥ -6 dB, refractive error ≤ 8.0 D and astigmatism ≤ 3 D. Eyes with evidence of retinal or neurological diseases or prior glaucoma surgery were excluded. All patients had at least one prior visual field before being enrolled in the study. Normal subjects were recruited by advertising at UCLA's campus, fliers in the clinics, and soliciting spouses and friends of patients seen at the Glaucoma Clinic, Jules Stein Eye Institute. The enrolled normal subjects were required to have open angles, corrected visual acuity of 20/25 or better, and normal eye exam including normal

visual fields and did not have definitive evidence of glaucomatous damage at the level of the optic nerve head (see below).

All subjects underwent a thorough eye exam on the day of imaging including visual acuity, automated refraction, IOP measurement, gonioscopy, slit lamp exam, dilated fundus exam, and standard achromatic perimetry (SAP) or short wavelength automated perimetry (SWAP) fields. Axial length and keratometry were measured by IOLMaster (Carl Zeiss-Meditec, Dublin CA). IOLMaster test results were considered reliable if the SN ratio for individual scans was above 3. Central corneal thickness (CCT) measurements were measured with a DGH 55 Pachmate (DGH Technology, Inc, Exton, PA). The device's output is the average of 10 reliable measurements of the central corneal thickness. Stereoscopic disc photographs and Optic Disc and Macular Cubes 200×200 (Cirrus HD-OCT) were carried out after pupillary dilation. All the images were reviewed afterwards by one of the investigators and images with signal strength <7, lost data on the peripapillary ring, obvious motion artifact, or incorrect segmentation were excluded.

The Optic Disc Cube 200×200 consists of 40,000 axial scans (in a 6×6×2 mm cube) centered on the optic disc. Average RNFL thickness and RNFL thickness in quadrants and clock hour sectors on a measurement circle 3.46 mm in diameter are calculated and their deviation from a normative database is provided in a color-coded scheme. RNFL pseudocolor thickness maps and deviation maps for the 6×6 mm area are also provided. The Macular Cube 200×200 algorithm measures 40,000 axial scans (in a 6×6×2 mm cube) centered on the fovea. The Ganglion Cell Analysis available on the Cirrus software version 6.0 (or higher) measures the combined thickness of the GCL and IPL in a 4.8×4.0 mm oval with longer horizontal axis. The GC/IPL layer is thickest in this area based on postmortem and in vivo measurements.^{9,11} Similar to other Cirrus printouts, it provides GC/IPL measurements in 6 wedge-shaped sectors after excluding the central foveolar region (1 mm in diameter) along with a pseudocolor scheme for the GC/IPL thickness. A deviation map also flags abnormally thin areas within the oval area as yellow ($p < 5\%$) or red ($p < 1\%$) superpixels.

Eyes with evidence of reproducible visual field loss consistent with glaucoma on SAP or SWAP visual fields regardless of IOP or disc appearance were considered to have glaucoma. Swedish Interactive Thresholding Algorithm (SITA) standard testing strategy was used for both SAP and SWAP tests. Only eyes with reliable visual fields (false positive rate of 15% or less) were included. Fixation loss and false negative error rates were not used as criteria for reliability for fields obtained on the day of enrollment.¹²⁻¹⁴ An abnormal SAP or SWAP visual field was defined as presence of a Glaucoma Hemifield Test (GHT) outside normal limits *and* presence of 4 abnormal test locations on pattern deviation plot with $p < 5\%$ both confirmed at least once. These criteria have been shown to be highly specific and demonstrated reasonable sensitivity for detection of early glaucomatous visual field loss.¹⁵ The visual fields were reviewed to exclude lid or lens artifacts.

The RNFL and GC/IPL thickness measurements from the Optic Disc and Macular 200×200 Cubes were exported to a personal computer. Factors potentially affecting the GC/IPL thickness in normal control subjects were explored with scatter plots, univariate regression, and two by two tables. We used spline methods and examined scatter plots to determine if the relationship between thickness measurements and the continuous predictors was linear. Average RNFL thickness, RNFL measurements in quadrants, RNFL thickness in 12 clock hour sectors, and average, minimum, and regional GC/IPL measurements were compared among the glaucoma and control groups.

Binary multivariate logistic regression analyses (backward stepwise) were carried out to adjust for the influence of covariates affecting the GC/IPL or RNFL measurements and correcting for potential correlation of the two eyes of the same subjects. Covariates were kept in the models if the p value was <0.15 . Average and regional RNFL and GC/IPL measurements were explored individually for discrimination of glaucoma patients from normal subjects. The sensitivity, specificity, and accuracy [accuracy = (sensitivity + specificity)/2] and areas under receiver operating characteristic (ROC) curves (AUCs), the coefficients for the partial AUCs, and their corresponding standard errors are reported.

The multivariate logistic regressions were adjusted for age, SD-OCT signal strength, disc size, and axial length. This regression was the basis of the adjusted ROC curves where the optimal threshold separating the two groups was allowed to vary depending on the covariates. We also explored potential interactions between diagnosis (normal vs. glaucoma) and the other covariates in the regression models. We investigated which of the above factors had an influence on thickness and computed the *adjusted* sensitivity, specificity, accuracy, and AUCs under this model. In addition to the total areas under the curves, we used partial areas under the ROC curves to compare performance of various parameters at high specificity (such as 95%). Positive and negative likelihood ratios (LR) were calculated for global and regional findings on the SD-OCT printouts to compare performance of various parameters as a function of the normative database of the Cirrus HD-OCT. The software Stata (version 12.1, StataCorp College Station, Texas, USA) was used for all data and statistical analyses.

Results

A total of 150 eyes of 99 subjects (59 eyes of 47 subjects with early perimetric glaucoma, and 91 control eyes belonging to 52 subjects) were enrolled. Table 1 describes the demographic characteristics of the study sample in detail. The control subjects were younger and had shorter axial length on average ($p < 0.001$ for both). On univariate analyses, the only factors found to be associated with thinner average RNFL thickness in the control group were older age ($p = 0.01$), longer axial length ($p = 0.012$), and potentially smaller disc area ($p = 0.073$) while the SD-OCT signal strength ($p = 0.305$) and spherical equivalent ($p = 0.344$) did not show any association with the average RNFL thickness. On multivariate analyses, older age (beta = -0.43μ per year; $p = 0.003$), longer axial length (beta = -2.11μ per mm; $p = 0.018$), and smaller disc area (beta = 1.19μ per 0.1 mm^2 ; $p = 0.056$) were associated with thinner average RNFL measurements in normal eyes.

Thinner global GC/IPL measurements in control subjects were associated with advancing age ($p = 0.001$), flatter keratometry ($p = 0.058$), longer axial length ($p = 0.101$), and male gender ($p = 0.149$) on univariate analyses in normal eyes. Signal strength did not show a significant association with average GC/IPL thickness ($p = 0.339$). On multivariate analyses, only age (beta = -0.28μ per year; $p = 0.001$) and axial length (beta = -1.36μ per mm; $p = 0.03$) predicted average GC/IPL thickness measurements in normal subjects. Interaction of age and axial length was not significant in multivariate analyses ($p = 0.140$). A lower average GC/IPL thickness predicted a worse MD in the normal control group (beta = $1.45\text{ dB per micron}$, $p = 0.017$) but the association disappeared after correcting for age and axial length. The average GC/IPL thickness significantly correlated with the average RNFL thickness in both the normal and glaucoma groups ($r = 0.693$ and $= 0.628$, respectively, $p < 0.001$ for both) (Figure 1) whereas the association with the disc area was not statistically significant ($r = 0.121$, $p = 0.252$ in the control group and $r = -0.020$ and $p = 0.876$ in the glaucoma group). No significant association was found between the average or regional GC/IPL thickness and average or regional outer retina thickness measurements ($r = -0.029$, $p = 0.801$ for normal

subjects and $r = -0.156$, $p = 0.251$ for glaucoma eyes for global measurements; $p > 0.05$ for all regional associations)(Figure 2).

Performance of the two algorithms for detection of glaucoma

Table 2 compares the global and regional/sectoral thickness measurements for RNFL and GC/IPL between the two groups and Figure 3 shows distribution of the difference between glaucoma and control groups for the average and regional GC/IPL and RNFL thickness measurements. All potentially significant covariates (i.e. parameters with $p < 0.15$ on univariate analyses, or factors that make biological sense, such as disc area) were included in the final stepwise multivariate analyses along with each global or regional RNFL or GC/IPL predictor and logit scores were calculated for each outcome for calculating AUCs. The final logistic models included age, signal strength, axial length, and disc size as covariates. The outer retina thickness or the ratio of GC/IPL to outer retina thickness was not a significant covariate in any of the global or regional multivariate models ($p > 0.6$ for all). The AUCs, sensitivities/specificities, and accuracies for the global and regional GC/IPL and RNFL thickness measures are presented in Table 3. As evident on Figures 4 and 5, the AUC for the average RNFL thickness was superior to average GC/IPL measurements (AUC = 0.964; 95% CI 0.936-0.991 vs. 0.937; 95% CI: 0.895-0.980; $p = 0.04$). The pAUC difference between the average RNFL and average GC/IPL thickness measurements with the cutoff point placed at 95% approached statistical significance ($p = 0.057$)(Figure 4). The performance of the minimum and inferotemporal GC/IPL thickness (the best performing regional GC/IPL measures) was similar to that of the inferior quadrant RNFL thickness, the best performing regional RNFL outcome [AUCs = 0.962 (95% CI: 0.915-0.985) vs. 0.955 (95% CI: 0.906-0.981) vs. 0.977 (95% CI: 0.943-0.996), $p = 0.71$ and $= 0.23$, respectively, p for pAUC difference of minimum and inferotemporal GC/IPL vs. the inferior quadrant RNFL = 0.77 and 0.82, respectively). When sensitivity and specificities were evaluated, the sensitivity for the minimum GC/IPL thickness or inferotemporal GC/IPL sector (81.3%, 95% CI: 70.9%-91.7% and 84.9%, 95% CI: 75.5%-94.3%, respectively) were comparable to but lower than that of the inferior quadrant RNFL (89.8%, 95% CI: 82.0-97.6%) when compared at high specificity (95%). As mentioned above, the ROC curves and sensitivities/specificities were all adjusted for confounding factors listed above. We also hypothesized that the adding the best regional GC/IPL parameter to the best regional RNFL parameter could potentially improve discrimination of glaucomatous from normal eyes although, given the very good performance of both parameters, a ceiling effect would be expected. We found that combining the two best GC/IPL and RNFL parameters actually improved the performance of the SD-OCT. The pseudo- R^2 for the logistic models improved from 0.655 to 0.756 and the partial AUC coefficient with the cutoff point at 95% specificity actually was better for the model including the combined parameters vs. the model including only the inferior quadrant (difference in observed pAUC coefficients: 0.005, 95% CI: 0.0002-0.010; $p = 0.041$)(Figure 6).

The sensitivities/specificities/accuracies and likelihood ratios for various RNFL and GC/IPL parameters are shown in Table 4 based on the statistical significance assigned by the Cirrus' normative database. Minimum GC/IPL (93.3%), inferior quadrant RNFL (92.0%) and inferotemporal GC/IPL (91.3%) had the highest accuracies (i.e., average of sensitivity and specificity). Overall, the average RNFL and GC/IPL measurements performed similarly and less adequately than regional measures. The RNFL clock hour sector thickness tended to have the highest false positive rate at 5% level (29.7%), while it had the highest positive LR at the 1% level (18.89, 95% CI: 7.20-49.60). An RNFL sector demonstrating $p > 5\%$ also had the best negative LR (0.05, 95% CI: 0.01-0.19) closely followed by the RNFL quadrant thickness and GC/IPL sectors (LR= 0.08, 95% CI: 0.03-0.20 and 0.11, 95% CI: 0.05-0.24), respectively.

Discussion

Interest in macular measurements for detection of glaucoma dates back more than a decade. Using Retinal Thickness Analyzer, Zeimer and colleagues were able to detect decreased macular thickness in eyes with established glaucoma.¹⁶ Similar findings were reported with earlier generations of OCT.¹⁷⁻²³ With the advent of SD-OCTs, the quality of OCT images has considerably improved allowing better segmentation and delineation of various macular layers. This has led to renewed interest in measuring the inner retinal layers where significant loss of cells occurs in glaucoma.^{24,25} Current SD-OCT devices have adopted different approaches in this regard. Initially, algorithms were developed to measure the combined thickness of the central macular RNFL, ganglion cell layer, and IPL called the ganglion cell complex or GCC.² Such measurements have shown very good reproducibility.²⁶ In Tan et al.'s study, the GCC global loss volume performed as well as the time-domain average RNFL. Ganglion cell complex measurements have been reported to be able to detect evidence of early damage in the seemingly noninvolved hemifield of glaucomatous eyes.²⁷ Seong et al. demonstrated that the GCC parameters performed as well as the RNFL thickness measurements in glaucoma eyes with early damage or eyes in which the visual field loss was within the central 10 degrees.²⁸ A review of the current literature with regard to GCC parameters demonstrates that performance of inner macular parameters approaches that of the RNFL although RNFL parameters still tend to carry out this task slightly better.^{2,28,29} This differential performance seems to be mostly a function of location of glaucomatous damage and the area of the macula scanned.^{28,30}

The goal of the current study was to fully evaluate the performance of the macular GC/IPL thickness measurements as determined by the most recent Cirrus HD-OCT software and compare its performance to that of circumpapillary RNFL thickness measurements for discrimination of eyes with early perimetric glaucoma (MD > -6.0 dB) from normal control eyes. We first evaluated the predictive factors determining the GC/IPL thickness in the normal control eyes. Specifically, we were interested in the potential correlation of the inner retina thickness with the outer retina thickness in the central macula. There are preliminary data that the ratio of the GCC to total retinal thickness (TRT) could potentially improve the discriminatory power of the SD-OCT measurements for detection of glaucoma.¹⁰

The global and regional GC/IPL thickness measurements diminished with advancing age and longer axial length. This is consistent with the available reports in the literature on this topic.^{9,31} We found no evidence of any potential correlations between the outer retina thickness and the GC/IPL measurements. When we entered either the absolute outer retina thickness or the ratio of the GC/IPL to outer retina thickness as covariates in multivariate logistic regression models, this finding was confirmed, i.e. neither covariate improved prediction of glaucoma when added to the multivariate models. This is in contrast to the findings by Kita and colleagues.¹⁰ They reported that the parameters average or superior or inferior GCC/TRT ratio actually outperformed the corresponding GCC parameters. Racial differences, difference in the axial length of the study samples, or the macular area examined may be partly responsible for the inconsistent findings. This may also be partly due to the fact that the RGCs do not directly overlie the corresponding rods and cones in the perifoveal area of the macula.³² One could argue that measuring macular or ganglion cell (GCC or GC/IPL) and outer retina volumes may be better indicators of the relationship between the inner and outer retinal layers. We are currently exploring this issue in further detail.

We then compared the performance of the GC/IPL thickness for detection of early glaucoma to that of RNFL thickness measurements after adjusting for relevant covariates such as age, axial length, OCT signal strength, and disc size. Our results showed that global RNFL

measurements (i.e. average RNFL thickness) were superior to global GC/IPL thickness values for detection of early glaucoma according to the AUC values; however, based on results provided by the normative database, the two global parameters actually demonstrated a similar performance. On the other hand, based on the AUC and partial AUC calculations, regional GC/IPL measurements (minimum (inferior quadrant). This finding suggests that in the macular region, similar to the GC/IPL and inferotemporal GC/IPL) performed as well as regional RNFL measurements peripapillary RNFL, early damage can be and often is localized. Alternatively, one may early localized loss. One important issue that needs to be emphasized is the fact that speculate that because of averaging, global measures are inherently less likely to detect macular SD-OCT imaging is actually measuring an area encompassing only half of the RGCs in the eye (in the central macula) whereas RNFL imaging aims to evaluate the entire complement of the RGC axons. The fact that the global RNFL measurements The enrolled group of glaucoma patients had early perimetric glaucoma with a median were superior to the corresponding GC/IPL measurements would be therefore expected. (IQR) MD of -2.4 (-3.6 to -1.1) dB and hence our findings are quite relevant for early detection or confirmation of glaucoma. We also found that combining the best RNFL early glaucomatous eyes from normal control eyes. This effect was evident when and GC/IPL parameters from Cirrus HD-OCT actually improved its ability to discriminate coefficients for partial AUCs at very high cutoff point for specificity (95%) were compared where it most matters (Figure 6). This means that despite the very good isolated performance of RNFL and GC/IPL parameters and the potential for a ceiling effect, combining best parameters from the two imaging algorithm could be of value for early detection of glaucoma although the clinical relevance of the magnitude of this effect may be debatable. The utility of combining various OCT parameters has been previously explored with both time-domain and spectral-domain OCTs.³³⁻³⁵ The study by Huang et al. used linear discriminant function for combining various OCT parameters. These findings need to be implemented in clinical software on current SD-OCT machines so that the full potential of combining various structural measures can be verified and used.

There are scant data in the literature as yet for performance of color probability maps of the GC/IPL printout. The high rate of false positive RNFL findings in myopic individuals is a well-known issue.³⁶ Our study is one of the first studies to explore the likelihood ratios for the Cirrus' GC/IPL parameters. As mentioned above, regional GC/IPL measures performed as well as those from RNFL although an abnormal RNFL clock sector at 1% significance level had the highest positive likelihood ratio and presence of a normal clock sector ($p > 5\%$) led to the highest negative likelihood ratio. It must be noted that the normative database of the Cirrus HD-OCT only takes into consideration the effect of aging and factors such as myopia and race are not accounted for. The latter could potentially have biased our findings since in contrast to AUCs derived from multivariate logistic regressions, the statistical significance of SD-OCT parameters could not be corrected for differences in clinical and demographic characteristics between the control and glaucoma groups.

Mwanza et al. recently explored the diagnostic performance of the new GC/IPL parameters and found that minimum and inferotemporal GC/IPL thickness measurements were the best parameters discriminating between eyes with early glaucoma (defined as eyes with MD > -6 dB similar to our study) and normal eyes and their performance was as good as peripapillary RNFL thickness measurements.⁶ Due to the varying inclusion criteria, SD-OCT devices used, and analysis algorithms, it is difficult to compare results across studies on this subject. The only available study comparing the utility of GCC vs. GC/IPL thickness measurements did not find a difference in the AUCs for these two parameters.⁷ Newly defined parameters such as global loss volume (GLV) and focal loss volume (FLV) have been designed to improve detection of early glaucoma with RTVue SD-OCT. The index GLV seems to be better suited to this aim based on data in the literature.^{2,37} However, most of the studies

based on the RTVue SD-OCT have looked at global GCC or GCC thickness in the superior or inferior hemiretina. In contrast, Cirrus HD-OCT provides regional GC/IPL measurements for detection of early glaucomatous damage. The minimum (followed by the inferotemporal) GC/IPL thickness had the best AUC among GC/IPL parameters, which was comparable to that of the inferior quadrant RNFL, the best regional parameter in the current study. The best regional RNFL and GC/IPL parameters for detection of early glaucoma were located both in the inferior hemifield (inferotemporal GC/IPL segment vs. inferior quadrant), which is consistent with the finding that the inferior rim is the most common site of early disc and RNFL glaucomatous damage.³⁸ Specifically, it has been recently shown that the inferior macular nerve fibers project to the inferior disc³⁹ and therefore it seems natural that the inferotemporal GC/IPL would perform as well as the inferior RNFL parameters. It has yet to be determined whether GC/IPL measurements have any advantage over GCC measurements for detection of early glaucoma⁷; but very good reproducibility for global and regional GC/IPL measurements has been reported.⁴⁰ This is consistent with other studies exploring reproducibility of various sublayers of the retina.^{2,41,42}

The current study enrolled consecutive subjects willing to participate in a tertiary setting and the glaucoma group tended to be somewhat older and had higher axial length. We addressed this issue by using multivariate analysis adjusting for potential differences in covariates.

In summary, we explored the performance of the GC/IPL parameters in a group of patients with early perimetric glaucoma and normal subjects. The findings confirm that inner macular parameters perform as well as RNFL parameters in such patients. We also found that combining the macular and RNFL data could potentially enhance SD-OCT's performance for detection of early glaucoma. The GCiPL/outer retina ratio did not enhance glaucoma detection in this study; however, this needs to be further explored.

Acknowledgments

a. Funding/Support: Research reported in this publication was supported by an award from Gerald Oppenheimer Family Foundation Center for Prevention of Eye Disease (KNM) and the National Eye Institute of Health under Award Number K23EY022659 (KNM).

b. Financial Disclosures:

Kouros Nouri-Mahdavi: Allergan, Consultant

Sara Nowroozizadeh: None

Nariman Nassiri: None

Nila Cirineo: None

Shane Knipping: None

JoAnn Giaconi: Allergan, Consultant

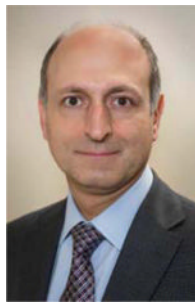
Joseph Caprioli: Allergan, Grant and Consultant; Merck, Grant; Alcon, Grant; New World Medical, Grant

d. Other Acknowledgments: Jeff Gornbein, DrPH, UCLA Department of Biomathematics, David Geffen School of Medicine, provided statistical assistance.

Biography



Sara Nowroozizadeh, MD, received her medical degree from Shiraz University of Medical Sciences, Shiraz, Iran, and finished her residency in Ophthalmology at Khalili Eye Hospital in the same University. She is currently an International Fellow at the Glaucoma Division, Stein Eye Institute, University of California Los Angeles.



Kouros Nouri-Mahdavi, MD, MSc, is Assistant Professor of Ophthalmology at the Glaucoma Division, Stein Eye Institute, University of California Los Angeles. His research interests include exploring functional tests for detection of glaucoma or its progression, enhancing the role of spectral-domain optical coherence tomography imaging in glaucoma, and the study of treatment outcomes in glaucoma.

References

1. Desatnik H, Quigley HA, Glovinsky Y. Study of central retinal ganglion cell loss in experimental glaucoma in monkey eyes. *J Glaucoma*. 1996; 5(1):46–53. [PubMed: 8795733]
2. Tan O, Chopra V, Lu AT, et al. Detection of macular ganglion cell loss in glaucoma by Fourier-domain optical coherence tomography. *Ophthalmology*. 2009; 116(12):2305–2314. e2301–2302. [PubMed: 19744726]
3. Kotera Y, Hangai M, Hirose F, Mori S, Yoshimura N. Three-dimensional imaging of macular inner structures in glaucoma by using spectral-domain optical coherence tomography. *Invest Ophthalmol Vis Sci*. 2011; 52(3):1412–1421. [PubMed: 21087959]
4. Lisboa R, Paranhos A Jr, Weinreb RN, Zangwill LM, Leite MT, Medeiros FA. Comparison of different spectral domain OCT scanning protocols for diagnosing preperimetric glaucoma. *Invest Ophthalmol Vis Sci*. 2013; 54(5):3417–3425. [PubMed: 23532529]
5. Nakano N, Hangai M, Nakanishi H, et al. Macular ganglion cell layer imaging in preperimetric glaucoma with speckle noise-reduced spectral domain optical coherence tomography. *Ophthalmology*. 2011; 118(12):2414–2426. [PubMed: 21924499]
6. Mwanza JC, Durbin MK, Budenz DL, et al. Glaucoma diagnostic accuracy of ganglion cell-inner plexiform layer thickness: comparison with nerve fiber layer and optic nerve head. *Ophthalmology*. 2012; 119(6):1151–1158. [PubMed: 22365056]

7. Kotowski J, Folio LS, Wollstein G, et al. Glaucoma discrimination of segmented cirrus spectral domain optical coherence tomography (SD-OCT) macular scans. *Br J Ophthalmol.* 2012; 96(11): 1420–1425. [PubMed: 22914498]
8. Kim NR, Kim JH, Lee J, Lee ES, Seong GJ, Kim CY. Determinants of perimacular inner retinal layer thickness in normal eyes measured by Fourier-domain optical coherence tomography. *Invest Ophthalmol Vis Sci.* 2011; 52(6):3413–3418. [PubMed: 21357406]
9. Mwanza JC, Durbin MK, Budenz DL, et al. Profile and Predictors of Normal Ganglion Cell-Inner Plexiform Layer Thickness Measured with Frequency Domain Optical Coherence Tomography. *Invest Ophthalmol Vis Sci.* 2011; 52(11):7872–7879. [PubMed: 21873658]
10. Kita Y, Kita R, Takeyama A, Takagi S, Nishimura C, Tomita G. Ability of Optical Coherence Tomography-determined Ganglion Cell Complex Thickness to Total Retinal Thickness Ratio to Diagnose Glaucoma. *J Glaucoma.* Jun 4.2012 [Epub ahead of print].
11. Curcio CA, Allen KA. Topography of ganglion cells in human retina. *J Comp Neurol.* 1990; 300(1):5–25. [PubMed: 2229487]
12. Bengtsson B, Heijl A. False-negative responses in glaucoma perimetry: indicators of patient performance or test reliability? *Am J Ophthalmol.* 2000; 130(5):689. [PubMed: 11078863]
13. Bengtsson B. Reliability of computerized perimetric threshold tests as assessed by reliability indices and threshold reproducibility in patients with suspect and manifest glaucoma. *Acta Ophthalmol Scand.* 2000; 78(5):519–522.
14. Junoy Montolio FG, Wesselink C, Gordijn M, Jansonius NM. Factors that influence standard automated perimetry test results in glaucoma: test reliability, technician experience, time of day, and season. *Invest Ophthalmol Vis Sci.* 2012; 53(11):7010–7017. [PubMed: 22952121]
15. Johnson CA, Sample PA, Cioffi GA, Liebmann JR, Weinreb RN. Structure and function evaluation (SAFE): I. criteria for glaucomatous visual field loss using standard automated perimetry (SAP) and short wavelength automated perimetry (SWAP). *Am J Ophthalmol.* 2002; 134(2):177–185. [PubMed: 12140023]
16. Zeimer R, Asrani S, Zou S, Quigley H, Jampel H. Quantitative detection of glaucomatous damage at the posterior pole by retinal thickness mapping. A pilot study. *Ophthalmology.* 1998; 105(2): 224–231. [PubMed: 9479279]
17. Bagga H, Greenfield DS, Knighton RW. Macular symmetry testing for glaucoma detection. *J Glaucoma.* 2005; 14(5):358–363. [PubMed: 16148583]
18. Guedes V, Schuman JS, Hertzmark E, et al. Optical coherence tomography measurement of macular and nerve fiber layer thickness in normal and glaucomatous human eyes. *Ophthalmology.* 2003; 110(1):177–189. [PubMed: 12511364]
19. Ishikawa H, Stein DM, Wollstein G, Beaton S, Fujimoto JG, Schuman JS. Macular segmentation with optical coherence tomography. *Invest Ophthalmol Vis Sci.* 2005; 46(6):2012–2017. [PubMed: 15914617]
20. Lederer DE, Schuman JS, Hertzmark E, et al. Analysis of macular volume in normal and glaucomatous eyes using optical coherence tomography. *Am J Ophthalmol.* 2003; 135(6):838–843. [PubMed: 12788124]
21. Wollstein G, Schuman JS, Price LL, et al. Optical coherence tomography (OCT) macular and peripapillary retinal nerve fiber layer measurements and automated visual fields. *Am J Ophthalmol.* 2004; 138(2):218–225. [PubMed: 15289130]
22. Tan O, Li G, Lu AT, Varma R, Huang D. Mapping of macular substructures with optical coherence tomography for glaucoma diagnosis. *Ophthalmology.* 2008; 115(6):949–956. [PubMed: 17981334]
23. Medeiros FA, Zangwill LM, Alencar LM, et al. Detection of glaucoma progression with stratus OCT retinal nerve fiber layer, optic nerve head, and macular thickness measurements. *Invest Ophthalmol Vis Sci.* 2009; 50(12):5741–5748. [PubMed: 19815731]
24. Glovinsky Y, Quigley HA, Pease ME. Foveal ganglion cell loss is size dependent in experimental glaucoma. *Invest Ophthalmol Vis Sci.* 1993; 34(2):395–400. [PubMed: 8440594]
25. Frishman LJ, Shen FF, Du L, et al. The scotopic electroretinogram of macaque after retinal ganglion cell loss from experimental glaucoma. *Invest Ophthalmol Vis Sci.* 1996; 37(1):125–141. [PubMed: 8550316]

26. Hirasawa H, Araie M, Tomidokoro A, et al. Reproducibility of Thickness Measurements of Macular Inner Retinal Layers Using SD-OCT With or Without Correction of Ocular Rotation. *Invest Ophthalmol Vis Sci.* 2013; 54(4):2562–2570. [PubMed: 23493298]
27. Takagi ST, Kita Y, Yagi F, Tomita G. Macular retinal ganglion cell complex damage in the apparently normal visual field of glaucomatous eyes with hemifield defects. *J Glaucoma.* 2012; 21(5):318–325. [PubMed: 21423034]
28. Seong M, Sung KR, Choi EH, et al. Macular and peripapillary retinal nerve fiber layer measurements by spectral domain optical coherence tomography in normal-tension glaucoma. *Invest Ophthalmol Vis Sci.* 2010; 51(3):1446–1452. [PubMed: 19834029]
29. Mori S, Hangai M, Sakamoto A, Yoshimura N. Spectral-domain optical coherence tomography measurement of macular volume for diagnosing glaucoma. *J Glaucoma.* 2010; 19(8):528–534. [PubMed: 20164794]
30. Morooka S, Hangai M, Nukada M, et al. Wide 3-dimensional macular ganglion cell complex imaging with spectral-domain optical coherence tomography in glaucoma. *Invest Ophthalmol Vis Sci.* 2012; 53(8):4805–4812. [PubMed: 22695956]
31. Koh VT, Tham YC, Cheung CY, et al. Determinants of ganglion cell-inner plexiform layer thickness measured by high-definition optical coherence tomography. *Invest Ophthalmol Vis Sci.* 2012; 53(9):5853–5859. [PubMed: 22836772]
32. Raza AS, Cho J, de Moraes CG, et al. Retinal ganglion cell layer thickness and local visual field sensitivity in glaucoma. *Arch Ophthalmol.* 2011; 129(12):1529–1536. [PubMed: 22159673]
33. Medeiros F, Zangwill L, Bowd C, Vessani R, Susannajr R, Weinreb R. Evaluation of retinal nerve fiber layer, optic nerve head, and macular thickness measurements for glaucoma detection using optical coherence tomography. *Am J Ophthalmol.* 2005; 139(1):44–55. [PubMed: 15652827]
34. Huang JY, Pekmezci M, Mesiwala N, Kao A, Lin S. Diagnostic power of optic disc morphology, peripapillary retinal nerve fiber layer thickness, and macular inner retinal layer thickness in glaucoma diagnosis with fourier-domain optical coherence tomography. *J Glaucoma.* 2011; 20(2): 87–94. [PubMed: 20577117]
35. Wang M, Lu AT, Varma R, Schuman JS, Greenfield DS, Huang D. Combining Information From 3 Anatomic Regions in the Diagnosis of Glaucoma With Time-Domain Optical Coherence Tomography. *J Glaucoma.* Jul 23.2012 [Epub ahead of print].
36. Aref AA, Sayyad FE, Mwanza JC, Feuer WJ, Budenz DL. Diagnostic Specificities of Retinal Nerve Fiber Layer, Optic Nerve Head, and Macular Ganglion Cell-Inner Plexiform Layer Measurements in Myopic Eyes. *J Glaucoma.* Dec 3.2012 [Epub ahead of print].
37. Nukada M, Hangai M, Mori S, et al. Imaging of Localized Retinal Nerve Fiber Layer Defects in Preperimetric Glaucoma Using Spectral-domain Optical Coherence Tomography. *J Glaucoma.* Oct 10.2012 [Epub ahead of print].
38. Jonas JB, Gusek GC, Naumann GO. [The parapapillary region of normal and glaucoma eyes. I. Planimetric values of 312 glaucoma and 125 normal eyes]. *Klin Monatsbl Augenh.* 1988; 193(1): 52–61.
39. Hood DC, Raza AS, de Moraes CG, Liebmann JM, Ritch R. Glaucomatous damage of the macula. *Prog Retin Eye Res.* 2013; 32:1–21. [PubMed: 22995953]
40. Mwanza JC, Oakley JD, Budenz DL, Chang RT, Knight OJ, Feuer WJ. Macular ganglion cell-inner plexiform layer: automated detection and thickness reproducibility with spectral domain-optical coherence tomography in glaucoma. *Invest Ophthalmol Vis Sci.* 2011; 52(11):8323–8329. [PubMed: 21917932]
41. Garas A, Vargha P, Hollo G. Reproducibility of retinal nerve fiber layer and macular thickness measurement with the RTVue-100 optical coherence tomograph. *Ophthalmology.* 2010; 117(4): 738–746. [PubMed: 20079538]
42. Arintawati P, Sone T, Akita T, Tanaka J, Kiuchi Y. The Applicability of Ganglion Cell Complex Parameters Determined From SD-OCT Images to Detect Glaucomatous Eyes. *J Glaucoma.* Jun 4.2012 [Epub ahead of print].

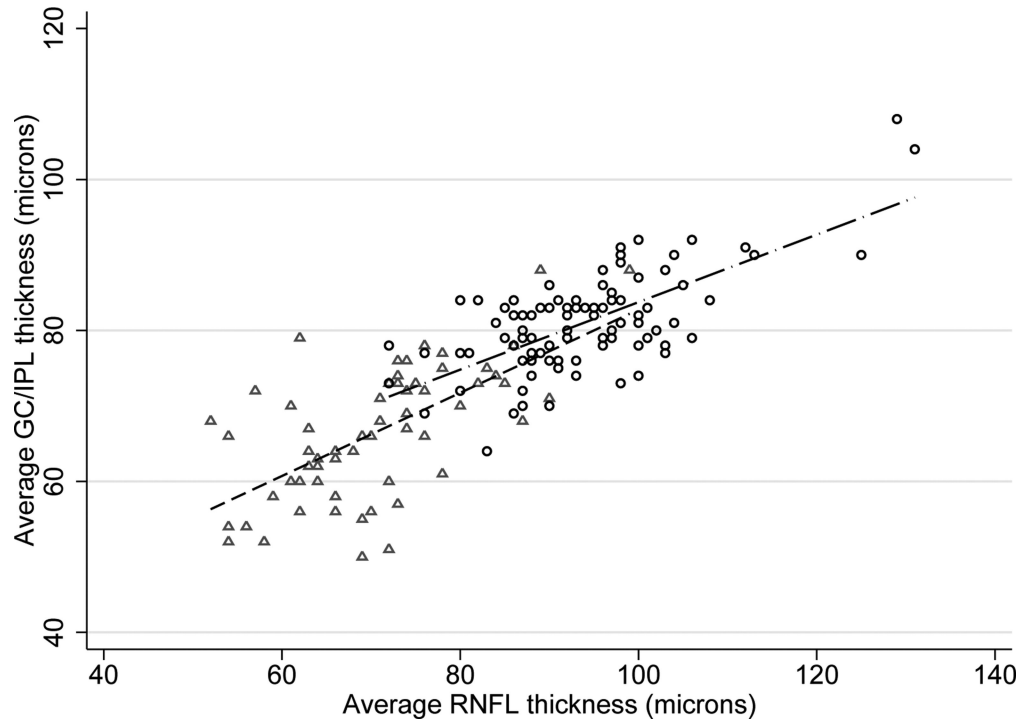


Figure 1. Association of the average ganglion cell/inner plexiform layer thickness with the average retinal nerve fiber layer thickness as a function of diagnosis. Circles: normal subjects, triangles: glaucoma patients.

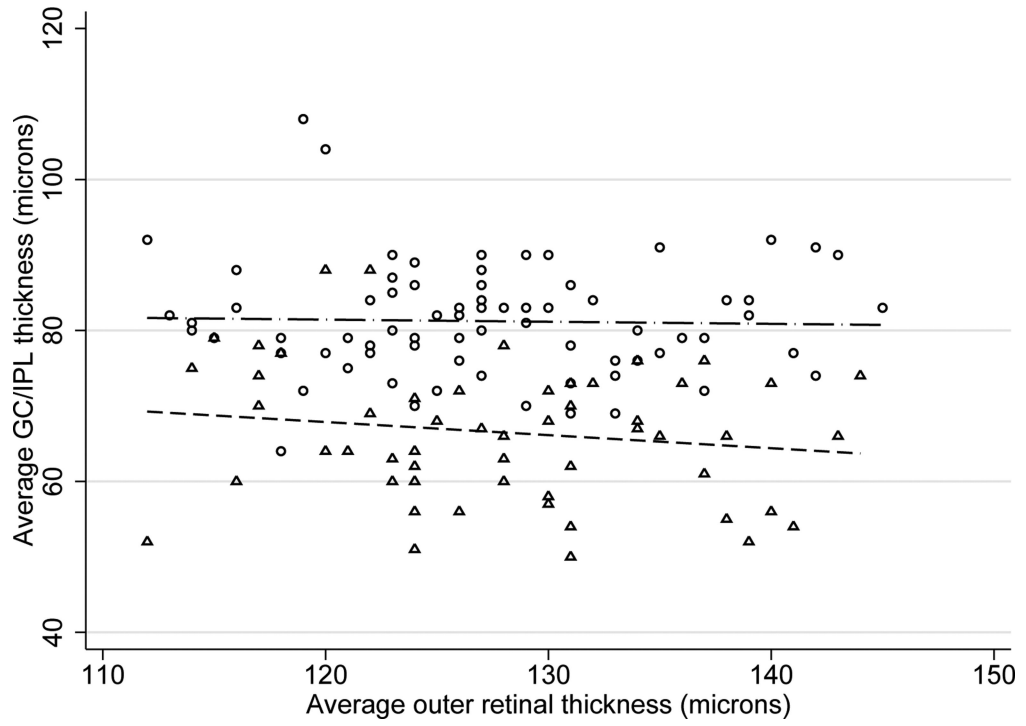


Figure 2. Association of the average ganglion cell/inner plexiform layer thickness with the average outer retinal thickness according to diagnosis. Circles: normal subjects, triangles: glaucoma patients.

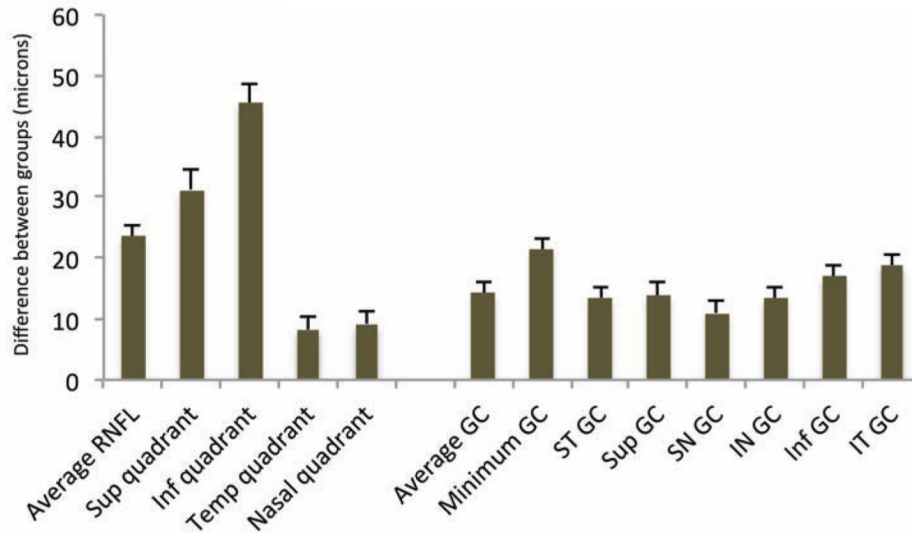


Figure 3. Bar graph demonstrates the average difference in the retinal nerve fiber layer and ganglion cell/inner plexiform layer parameters in the glaucoma and control groups. Whiskers represent one standard error. GC: ganglion cell/IPL thickness; ST: superotemporal, SN: superonasal, IN: inferonasal, IT: inferotemporal.

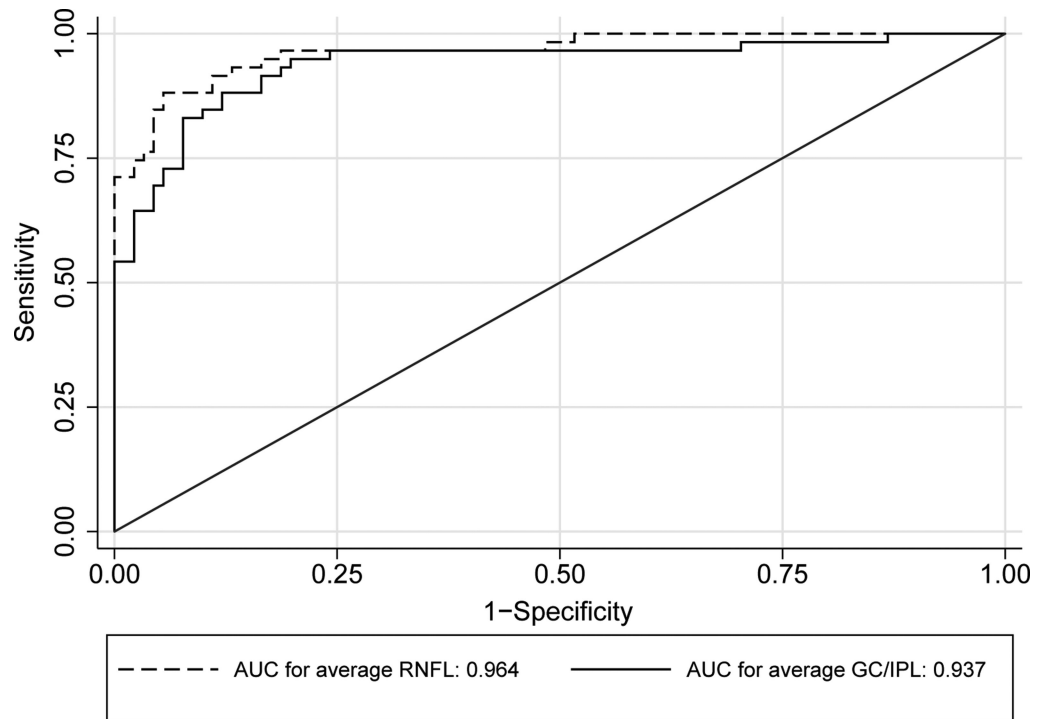


Figure 4. Receiver operating characteristic curves comparing performance of average retinal nerve fiber layer and ganglion cell/inner plexiform layer thickness measurements for detection of early perimetric glaucoma.

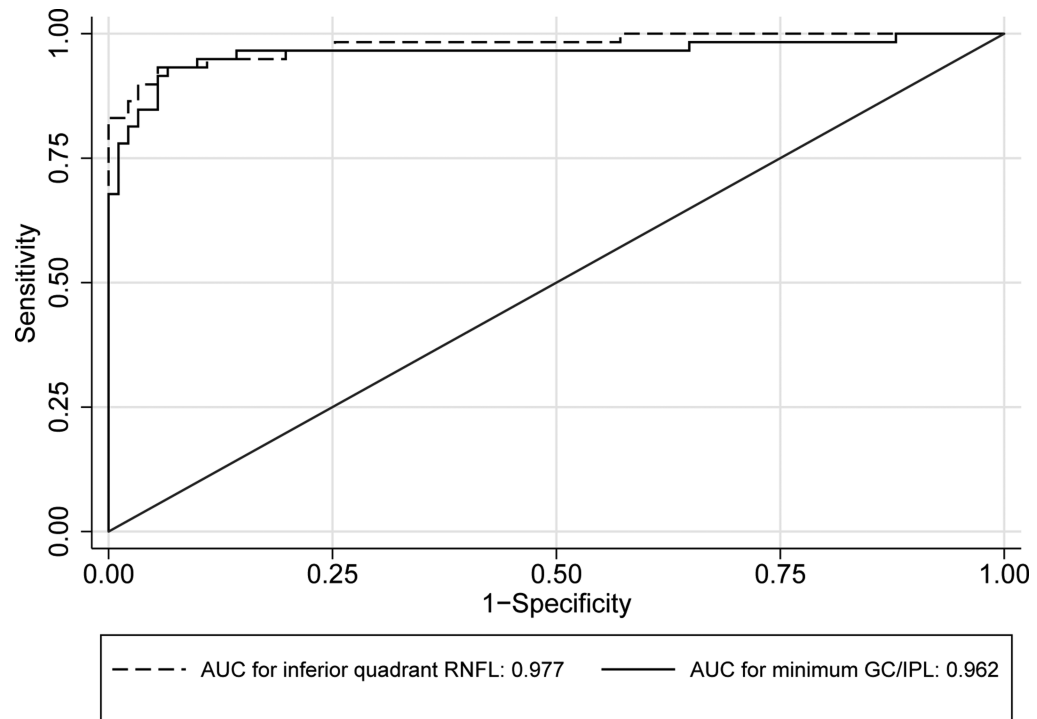


Figure 5. Receiver operating characteristic curves comparing performance of the best retinal nerve fiber layer parameter (inferior quadrant thickness) and the best ganglion cell/inner plexiform (GC/IPL) layer parameter (minimum GC/IPL) for detection of early perimetric glaucoma.

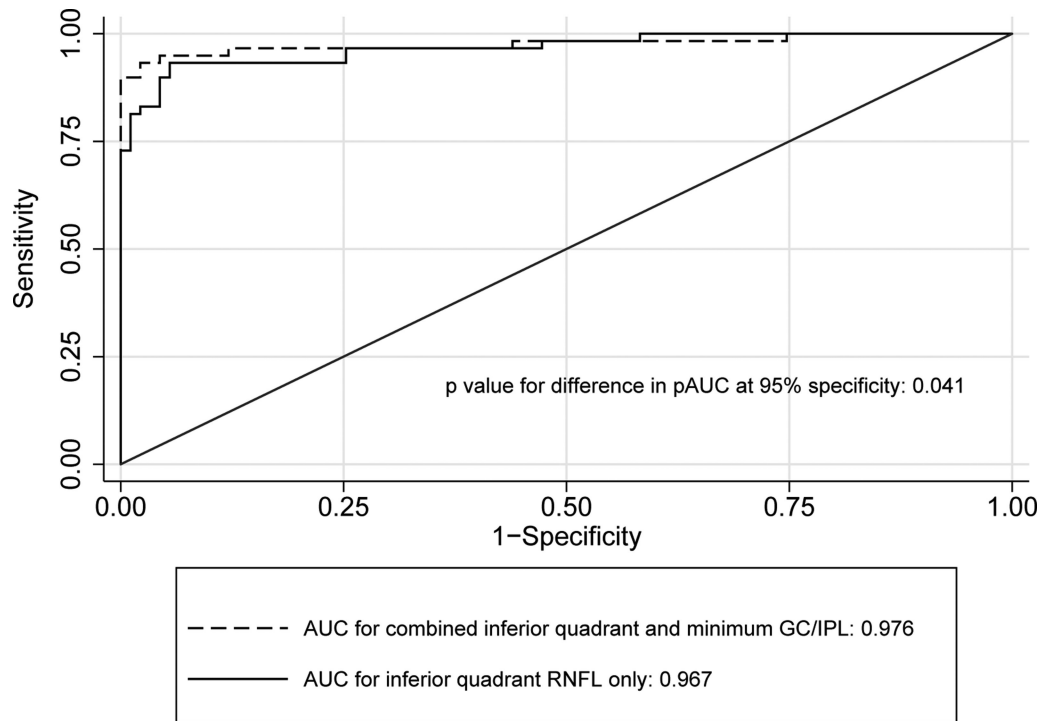


Figure 6. Receiver operating characteristic curves comparing performance of the inferior quadrant thickness alone (best retinal nerve fiber layer parameter) with the combined performance of the inferior quadrant and the minimum ganglion cell/inner plexiform layer thickness for detection of early perimetric glaucoma.

Table 1

Demographic and clinical characteristics of the study sample according to diagnosis in 150 eyes of 99 subjects enrolled to compare the performance of the retinal nerve fiber and ganglion cell/inner plexiform layer measurements with spectral domain optical coherence tomography for detection of early glaucoma.

Variables	Normal subjects	Glaucoma patients	P value
Number of eyes (patients)	91 (52)	59 (47)	
Age (mean \pm SD, years)	58.6 (\pm 9.2)	66.1 (\pm 6.0)	<0.001 ^a
Gender (female/male)	58/33	36/23	0.737 ^b
Race			
White	39 (75.0%)	36 (76.6%)	0.620 ^b
African-American	4 (7.7%)	6 (12.8%)	
Hispanic	3 (5.8%)	2 (4.3%)	
Asian	6 (11.5%)	3 (6.4%)	
LogMAR visual acuity (mean \pm SD)	0.0 (\pm 0.1)	0.1 (\pm 0.1)	0.061 ^a
Refractive error (Diopters, mean \pm SD)	-0.4 (\pm 2.4)	-1.2 (\pm 2.6)	0.154 ^a
IOP (mmHg, mean \pm SD)	14.7 (\pm 2.9)	14.1 (\pm 3.8)	0.314 ^a
Central corneal thickness (μ m, mean \pm SD)	556.1 (\pm 38.9)	548.8 (\pm 35.5)	0.323 ^a
Keratometry (Diopters, mean \pm SD)	44.2 (\pm 1.5)	43.9 (\pm 1.4)	0.260 ^a
Lens status			
Phakic	91 (100%)	42 (71.2%)	<0.001 ^b
Pseudophakic	0 (0%)	17 (28.8%)	
Axial length (mm, mean \pm SD)	23.8 (\pm 1.1)	24.7 (\pm 1.2)	<0.001 ^a
Signal Strength Macular Cube (mean \pm SD)	8.7 (\pm 1.0)	8.3 (\pm 0.8)	0.010 ^c
Signal Strength Optic Disc Cube (mean \pm SD)	8.8 (\pm 1.0)	8.0 (\pm 0.8)	<0.001 ^c
Disc area (mm ² , mean \pm SD)	1.73 (\pm 0.3)	1.73 (\pm 0.4)	0.922 ^a
Mean deviation (dB, mean \pm SD)	-0.1 (\pm 1.2)	-2.5 (\pm 1.9)	<0.001 ^c
Pattern standard deviation (dB, mean \pm SD)	1.6 (\pm 0.4)	4.5 (\pm 2.2)	<0.001 ^c

^aTwo-sample t test

^bChi² test

^cWilcoxon's rank-sum test; **SD**: standard deviation; **LogMAR**: logarithm of minimum angle of resolution; **IOP**: intraocular pressure.

Table 2

Comparison of global and regional ganglion cell/inner plexiform layer (GC/IPL), macular, and RNFL thickness measurements in the control and early perimetric glaucoma groups.

OCT parameters	Normal group	Glaucoma subjects	P value
GC/IPL parameters			
<i>Average GC (mean ± SE)</i>	81.1 (±1.0)	66.5 (±1.3)	<0.001
<i>Minimum GC (mean ± SE)</i>	79.2 (±0.9)	57.8 (±1.4)	<0.001
<i>Superotemporal GC (mean ± SE)</i>	80.5 (±0.9)	66.9 (±1.4)	<0.001
<i>Superior GC (mean ± SE)</i>	81.8 (±1.0)	67.9 (±1.7)	<0.001
<i>Superonasal GC (mean ± SE)</i>	82.3 (±1.1)	71.2 (±1.8)	<0.001
<i>Inferonasal GC (mean ± SE)</i>	80.6 (±1.0)	67.2 (±1.7)	<0.001
<i>Inferior GC (mean ± SE)</i>	79.9 (±1.0)	63.1 (±1.4)	<0.001
<i>Inferotemporal GC (mean ± SE)</i>	81.7 (±0.9)	62.9 (±1.4)	<0.001
RNFL parameters			
<i>Average RNFL (mean ± SE)</i>	94.0 (±1.1)	70.5 (±1.3)	<0.001
<i>Superior quadrant (mean ± SE)</i>	115.7 (±1.7)	84.3 (±2.4)	<0.001
<i>Nasal quadrant (mean ± SE)</i>	72.9 (±1.2)	63.6 (±1.2)	<0.001
<i>Inferior quadrant (mean ± SE)</i>	124.0 (±1.9)	78.6 (±2.1)	<0.001
<i>Temporal quadrant (mean ± SE)</i>	63.5 (±1.2)	55.5 (±1.5)	<0.001
<i>1 o'clock sector (mean ± SE)</i>	104.8 (±2.3)	79.7 (±2.7)	<0.001
<i>2 o'clock sector (mean ± SE)</i>	89.7 (±1.9)	76.5 (±3.7)	<0.001
<i>3 o'clock sector (mean ± SE)</i>	61.7 (±1.2)	58.9 (±1.3)	0.021
<i>4 o'clock sector (mean ± SE)</i>	66.5 (±1.3)	58.6 (±1.3)	<0.001
<i>5 o'clock sector (mean ± SE)</i>	100.9 (±2.4)	74.7 (±2.3)	<0.001
<i>6 o'clock sector (mean ± SE)</i>	136.6 (±2.8)	86.3 (±3.2)	<0.001
<i>7 o'clock sector (mean ± SE)</i>	134.3 (±2.7)	74.9 (±3.4)	<0.001
<i>8 o'clock sector (mean ± SE)</i>	62.7 (±1.5)	55.2 (±1.8)	0.008
<i>9 o'clock sector (mean ± SE)</i>	51.4 (±1.1)	49.8 (±1.4)	0.417
<i>10 o'clock sector (mean ± SE)</i>	76.8 (±1.6)	61.5 (±2.2)	<0.001
<i>11 o'clock sector (mean ± SE)</i>	124.8 (±2.3)	89.7 (±3.1)	<0.001
<i>12 o'clock sector (mean ± SE)</i>	117.8 (±2.8)	83.6 (±3.0)	<0.001

OCT: Optical Coherence Tomography; **RNFL:** Retinal Nerve Fiber Layer; **GC:** Ganglion Cell; **GC/IPL:** Ganglion Cell/Inner Plexiform Layer.

Table 3

Area under the receiver operating characteristic curves for retinal nerve fiber and ganglion cell/inner plexiform layer parameters as measured with spectral domain optical coherence tomography.

	AUC (95% CI)	Sensitivity	Specificity	Accuracy		AUC (95% CI)	Sensitivity	Specificity
RNFL parameters								
<i>Average RNFL</i>	0.964 (0.936-0.991)	88.1%	91.2%	90.0%				
<i>Superior quadrant</i>	0.936 (0.898-0.974)	84.8%	86.8%	86.0%	<i>Nasal quadrant</i>	0.889 (0.837-0.942)	74.6%	85.7%
<i>Inferior quadrant</i>	0.976 (0.952-0.999)	93.2%	91.2%	92.0%	<i>Temporal quadrant</i>	0.880 (0.826-0.933)	71.2%	82.4%
<i>1 o'clock sector</i>	0.896 (0.844-0.947)	81.4%	83.5%	82.4%	<i>2 o'clock sector</i>	0.875 (0.815-0.936)	93.2%	80.2%
<i>3 o'clock sector</i>	0.866 (0.809-0.923)	83.1%	80.2%	81.6%	<i>4 o'clock sector</i>	0.877 (0.821-0.932)	88.1%	75.8%
<i>5 o'clock sector</i>	0.906 (0.858-0.953)	91.5%	75.8%	83.7%	<i>6 o'clock sector</i>	0.952 (0.917-0.987)	91.5%	86.8%
<i>7 o'clock sector</i>	0.964 (0.933-0.995)	93.2%	93.4%	93.3%	<i>8 o'clock sector</i>	0.867 (0.810-0.923)	96.6%	62.6%
<i>9 o'clock sector</i>	0.861 (0.802-0.920)	81.4%	82.4%	81.9%	<i>10 o'clock sector</i>	0.898 (0.847-0.949)	91.5%	76.9%
<i>11 o'clock sector</i>	0.919 (0.876-0.961)	88.1%	82.4%	85.3%	<i>12 o'clock sector</i>	0.907 (0.860-0.955)	81.4%	90.1%
GC/IPL parameters								
<i>Average GC/IPL</i>	0.937 (0.889- 0.972)	86.4%	87.9%	87.3%	<i>Minimum GC/IPL</i>	0.962 (0.915-0.985)	91.5%	94.5%
<i>Superior GC/IPL</i>	0.906 (0.848-0.948)	76.3%	86.8%	85.0%	<i>Inferior GC/IPL</i>	0.938 (0.889-0.972)	83.1%	91.2%
<i>Inferonasal GC/IPL</i>	0.891 (0.833-0.938)	72.9%	82.4%	78.7%	<i>Superotemporal GC/IPL</i>	0.926 (0.873-0.963)	83.3%	74.6%
<i>Inferotemporal GC/IPL</i>	0.955 (0.906-0.981)	86.4%	94.5%	91.3%	<i>Superonasal GC/IPL</i>	0.871 (0.809-0.922)	71.2%	83.5%

OCT: Optical Coherence Tomography; **RNFL:** Retinal Nerve Fiber Layer; **GC/IPL:** Ganglion Cell/Inner Plexiform Layer; **AUC:** Area Under Curve.

Table 4

Frequency of statistically abnormal measurements as flagged on the retinal nerve fiber layer and Ganglion Cell Analysis printouts of Cirrus high-definition optical coherence tomography in the normal control subjects and glaucoma patients.

OCT parameters	Normal group		Glaucoma group		Positive Likelihood Ratio		Negative Likelihood Ratio	
	<i>p</i> <5%	<i>p</i> <1%	<i>p</i> <5%	<i>p</i> <1%	<i>p</i> <5%	<i>p</i> <1%	<i>p</i> <5% considered abnormal	Only <i>p</i> <1% considered abnormal
Average RNFL	10 (11%)	8 (8.8%)	42 (71.2%)	25 (42.4%)	6.47 (3.53-11.88)	4.82 (2.33-9.96)	0.32 (0.22-0.49)	0.63 (0.50-0.79)
Average GC/IPL	10 (11%)	5 (5.5%)	37 (62.7%)	30 (50.9%)	5.71 (3.08-10.6)	9.25 (3.81-22.50)	0.42 (0.30-0.59)	0.52 (0.40-0.68)
RNFL quadrant	11(12.1%)	9 (9.9%)	55 (93.2%)	49 (83.1%)	7.71 (4.41-13.49)	8.39 (4.47-15.78)	0.08 (0.03-0.20)	0.18 (0.11-0.33)
RNFL sectors	27(29.7%)	4 (4.4%)	57 (96.6%)	49 (83.1%)	3.25 (2.37-4.48)	18.89 (7.2-49.60)	0.05 (0.01-0.19)	0.18 (0.10-0.31)
GC/IPL sectors	8 (8.8%)	6 (6.6%)	53 (89.8%)	49 (83.1%)	10.22 (5.24-19.92)	12.60 (5.76-27.53)	0.11 (0.05-0.24)	0.18 (0.10-0.32)
Min GC/IPL	7 (7.7%)	6 (6.6%)	50 (84.8%)	42 (71.2%)	11.02 (5.36-22.63)	10.80 (4.90-23.79)	0.16 (0.09-0.30)	0.30 (0.21-0.46)

OCT: Optical Coherence Tomography; **RNFL:** Retinal Nerve Fiber Layer; **GC/IPL:** Ganglion Cell/inner plexiform layer; **Min:** Minimum.